

AZIMUTHALLY-DEPENDENT FINITE ELEMENT SOLUTION TO THE CYLINDRICAL RESONATOR*

Roberto A. Osegueda, Joseph H. Pierluissi, Luis M. Gil,
Arturo Revilla and Gustavo J. Villalva
The University of Texas at El Paso
College of Engineering
El Paso, TX 79968

and

G. John Dick, David G. Santiago and Rabi T. Wang
Jet Propulsion Laboratory
California Institute of Technology
Pasadena, CA 91009

Abstract: The cylindrical cavity resonator loaded with an anisotropic dielectric is analyzed as a two-dimensional problem using a finite element approach that assumes sinusoidal dependence in azimuth. This methodology allows the first finite element treatment of the technically important case of a resonator containing a sapphire element with a cylindrically aligned c axis. Second order trial functions together with quadrilateral elements are adopted in the calculations. The method was validated through comparisons with the analytical solutions for the hollow metal cavity and a coaxial cavity, as well as through measurements on a shielded sapphire resonator.

1. Introduction

Although the analytical determination of resonant modes and frequencies of the metallic cylindrical cavity has a well established history, a solution for the cavity partially filled with an anisotropic dielectric generally requires computationally complex, three-dimensional numerical analyses. Approximate analytical means of analyzing the dielectric resonator have been proposed throughout the years [1, 2], and with some degree of accuracy the theoretical estimates have agreed well with experimental results. However, because of the inherent shortcomings of the approximate analytical models, numerical methods have continued to receive a great deal of attention during the past years [3, 4].

Recently, so called "whispering gallery" resonators consisting of a sapphire dielectric element in a metallic container have made possible new capabilities for microwave oscillator phase noise and frequency stability [5,6]. With high azimuthal mode numbers, these resonators isolate radio-frequency energy to the dielectric element and away from the metallic

* This work was sponsored by and carried out in part at Jet Propulsion Laboratory, California Institute of Technology, under a contract with the National Aeronautics and Space Administration.

container, thus providing extraordinary low losses and high quality factors (Q's). However, these widely disparate field magnitudes pose a challenge for any methodology to accurately calculate (e.g.) conductive losses due to small evanescent fields at the wall of the containing can. In particular, a three-dimensional finite element method allowing full treatment of sapphire's anisotropic dielectric constant, would require such a large number of nodes as to become impractical. Analytical methods are unattractive, with new approaches required for every geometrical configuration change. A two-dimensional finite element approach, however, would allow easy treatment of any cylindrically symmetric resonator geometry.

Because the dielectric constant for sapphire shows cylindrical symmetry, a two dimensional treatment is allowed for the important case where its crystal c axis is aligned with a physical axis of axisymmetry. In terms of the field intensities, the problem is governed by the three-component vector Helmholtz equation which can be treated as an axisymmetric problem only for modes with no azimuthal (or ϕ) dependence. Such zero-order modes can be obtained from a two-dimensional approach to the cavity in the r-z plane using a variety of techniques which yield reasonable accuracy. Higher order solution for isotropic dielectrics are still obtainable in two dimensions if the azimuthal dependence of the modes is assumed *a priori* [7]. In the work presented here, the authors reduce the finite element analysis of the anisotropic dielectric resonator to two dimensions by assuming an exponential ϕ -dependence, and limiting the permittivity tensor to possess longitudinal and transverse components only. While ruling out most anisotropic dielectric configurations, this approach makes possible the first two-dimensional finite element treatment for sapphire "whispering gallery" resonators.

II. Fundamental Equations

In terms of the magnetic field intensity \mathbf{H} , the vector Helmholtz equation with the penalty term included is given by [8]

$$\nabla \times [\mathbf{k}]^{-1} \nabla \times \mathbf{H} - \alpha \nabla (\nabla \cdot \mathbf{H}) - k_0^2 \mathbf{H} = \mathbf{0} \quad (1)$$

in which $[\mathbf{k}]$ is the tensor dielectric constant, α is an empirical coefficient of the penalty term $\nabla (\nabla \cdot \mathbf{H})$, and k_0 is the free-space propagation constant. The variational energy functional associated with (1) is given by [8]

$$F\{\mathbf{H}\} = \int_{\Omega} \{ (\nabla \times \mathbf{H}) \cdot ([\mathbf{k}]^{-1} \nabla \times \mathbf{H}) - k_0^2 \mathbf{H} \cdot \mathbf{H} + \alpha (\nabla \cdot \mathbf{H}) \cdot (\nabla \cdot \mathbf{H}) \} d\Omega \quad (2)$$

where Ω is the volume of the resonator. In a finite element solution, \mathbf{H} is normally chosen instead of \mathbf{E} because of the discontinuity of the latter at dielectric interfaces.

At the interface between a perfect conductor and a lossless dielectric with a unit normal vector \mathbf{a}_n the use of (2) implies that

$$\mathbf{a}_n \times [\mathbf{k}]^{-1} (\nabla \times \mathbf{H}) = 0 \quad , \quad (3)$$

as a naturally satisfied condition, while the condition

$$\mathbf{a}_n \cdot \mathbf{H} = 0 \quad , \quad (4)$$

needs to be enforced. There is no axis of axisymmetry for the higher order modes ($n > 0$) and, hence, no perfect magnetic conductor with its associated boundary condition needs to be invoked along the z axis.

III. Finite Element Analysis

Inside the volume of the cylindrical resonator the magnetic field vector maybe described as

$$\left\{ \begin{array}{l} H_r(r, \phi, z) \\ H_\phi(r, \phi, z) \\ H_z(r, \phi, z) \end{array} \right\} = \left[\begin{array}{l} H_r(r, z) \\ H_\phi(r, z) \\ H_z(r, z) \end{array} \right] e^{jn\phi} \quad , \quad (5)$$

where

$$\left\{ \mathbf{H}(r, z) \right\}^T = \left[H_r(r, z) \quad j H_\phi(r, z) \quad H_z(r, z) \right] \quad , \quad (6)$$

and $H_r(r, z)$, $H_\phi(r, z)$ and $H_z(r, z)$ are functions describing the variations of the components of the field vectors in the r-z plane. The n in (5) denotes the azimuthal mode number (1, 2, 3, . . .) while j is used to establish the component H_ϕ to be in phase quadrature with the transverse components H_r and H_z . In this manner, $H_r(r, z)$, $H_\phi(r, z)$ and $H_z(r, z)$ are real functions.

This finite element formulation considers the use of general ring elements to solve for the magnetic field vectors. These elements are defined in the r-z plane and have m nodes. Within each finite element, $\mathbf{H}(r, z)$ is approximated in terms of the standard shape function matrix $[\mathbf{N}]$ as

$$\left\{ \mathbf{H}(r, \phi, z) \right\} = [\mathbf{N}(r, z)]^T \left\{ \mathbf{H} \right\}_e e^{jn\phi} \quad , \quad (7)$$

in which

$$[\mathbf{N}(r, z)] = \left[\begin{array}{ccc} \{ \mathbf{N}(r, z) \} & \{ 0 \} & \{ 0 \} \\ \{ 0 \} & j \{ \mathbf{N}(r, z) \} & \{ 0 \} \\ \{ 0 \} & \{ 0 \} & \{ \mathbf{N}(r, z) \} \end{array} \right] \quad , \quad (8)$$

$$\{ N(r,z) \}^T = [N_1(r,z) \ N_2(r,z) \ \dots \ N_m(r,z)] \quad (9)$$

and

$$\{H\}_e = \left[\{H_r\}_e^T \{H_\phi\}_e^T \{H_z\}_e^T \right]^T \quad (10)$$

Here, $\{H\}_e$ is a collection **matrix** of order $3m$ by 1 containing the unknown **nodal values** of the field arranged as in (10), and $N_i(r,z)$ is the shape function associated with the i^{th} node of the element. The specification of the azimuthal dependence in (7) allows for a trivial analytical integration of the functional in (2) from $\phi=0$ to $\phi=2\pi$ when the dielectric properties are ϕ -independent.

The substitution of the field approximation in (7) into the functional expression (2) leads to the element matrix equation

$$F_e = \{H\}_e^T \left[[S]_e + [U]_e - k_0^2 [T]_e \right] \{H\}_e, \quad (11)$$

where

$$[S]_e = \int_{\Omega} [A]^* [K]^{-1} [A]^T d\Omega, \quad (12)$$

$$[U]_e = \int_{\Omega} [C]^* [C]^T d\Omega, \quad (13)$$

$$[T]_e = \int_{\Omega} [N]^* [N]^T d\Omega, \quad (14)$$

$$[A] = e^{jn\phi} \begin{vmatrix} \{0\} & \left\{ \frac{\partial N}{\partial z} \right\} & -j \frac{n}{r} \{N\} \\ \left\{ \frac{\partial N}{\partial z} \right\} & \{0\} & j \frac{1}{r} \{N\} + j \left\{ \frac{\partial N}{\partial r} \right\} \\ j \frac{n}{r} \{N\} & -\left\{ \frac{\partial N}{\partial r} \right\} & \{0\} \end{vmatrix} \quad (15)$$

and

$$[C] = e^{jn\phi} \begin{vmatrix} \left(\frac{1}{r} + \frac{\partial}{\partial r}\right)\{N\} \\ -\frac{n}{r}\{N\} \\ \frac{\partial}{\partial z}\{N\} \end{vmatrix} \quad (16)$$

The integrations of (12), (13) and (14) over the azimuthal direction are done analytically, requiring that the dielectric properties $[K]$ in (12) be ϕ -independent. This is satisfied when $[K]$ has zero value off diagonal coefficients, and when the radial permittivity is equal to the azimuthal permittivity. The integrations of (12), (13) and (14) over the element area in the r - z plane are evaluated numerically using the standard Gauss-quadrature technique generally used for isoparametric elements with non-rectangular and curved shapes [9].

The global form of the functional in (11) may be expressed symbolically as

$$F = \{H\}^T \left[[S] + [U] - k_0^2 [T] \right] \{H\} \quad , \quad (17)$$

where $[S]$, $[U]$ and $[T]$ are global matrices resulting from the superposition of the corresponding element matrices, and $\{H\}$ contains all the unknown nodal values of the magnetic field vector.

Applying the Rayleigh-Ritz criterion, (17) "yields the eigenvalue equation

$$\left[[S] + [U] \right] \{H\} - k_0^2 [T] \{H\} = 0 \quad , \quad (18)$$

which needs to be solved for the resonant frequencies $\omega_r = ck_0$ and for the nodal values of the corresponding mode intensities $\{H\}$. The parameter c is the velocity of light in free space.

IV. Comparison to Analytical Solution

The proposed method was tested by solving for the resonant frequencies and modes of a metallic hollow, cylindrical cavity resonator with a radius of 3.8 cm and a height of 4.5 cm since the exact analytical solution is well-known. The resonator was modeled using rectangular ring elements with four corner nodes and bilinear shape functions. Solutions were obtained using 16, 36, 64 and 100 elements. A penalty factor of $\alpha = 1$ was assumed in (1) throughout the calculations. The identification of the modes and the removal of spurious modes was assisted by computations of the cosine of the angle β between the eigenvectors from the finite element solution and the exact eigenvectors. The cosine of this angle is given by [8] as:

where $\{H\}$ is the eigenvector solution of (18), $\{H_a\}$ are the nodal values calculated from the exact analytical expressions, and the factors in the denominator are Euclidian norms. If the

$$\cos \beta = \frac{\{H\}^T \{H_a\}}{\|\{H\}\|_2 \|\{H_a\}\|_2} \quad (19)$$

value of $\cos \beta$ in (19) is close to one or minus one, then the field vectors $\{H\}$ and $\{H_a\}$ are the same. Equation (19) was evaluated using each $\{H_a\}$ and all $\{H\}$ vectors to find the correspondence between each analytical vector and the numerical eigenvector.

Figure 1 shows convergence curves for ω_r obtained from the finite element solution for the transverse magnetic TM_{6ml} series modes, where the subscripts represent the number of oscillations in ϕ , r , and z , respectively. The abscissa corresponds to the order of mode extraction in the finite element solution. For 100 elements the resonant frequencies converged to about 0,12% from the exact values for both the TE and TM modes, Fig. 2 shows a sample of the results obtained through the use of the cosine of the angle between vectors in (19) for mode identification. The true TE_{0ml} modes are shown on the top of the figure, with a cosine close to one, while the spurious modes have values much lower than one. Fig. 3 shows the frequencies of various families of TE and TM modes of the cavity resonator as functions of the azimuthal index.

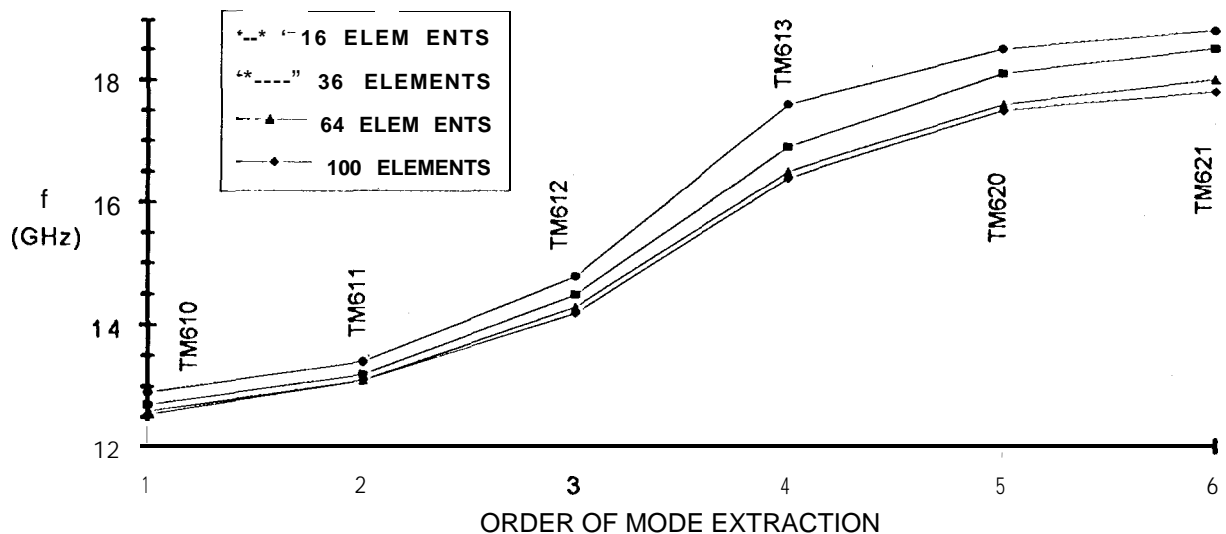


Figure 1. Convergence curves of the finite element frequencies for the first six modes of the hollow cavity with $n=6$.

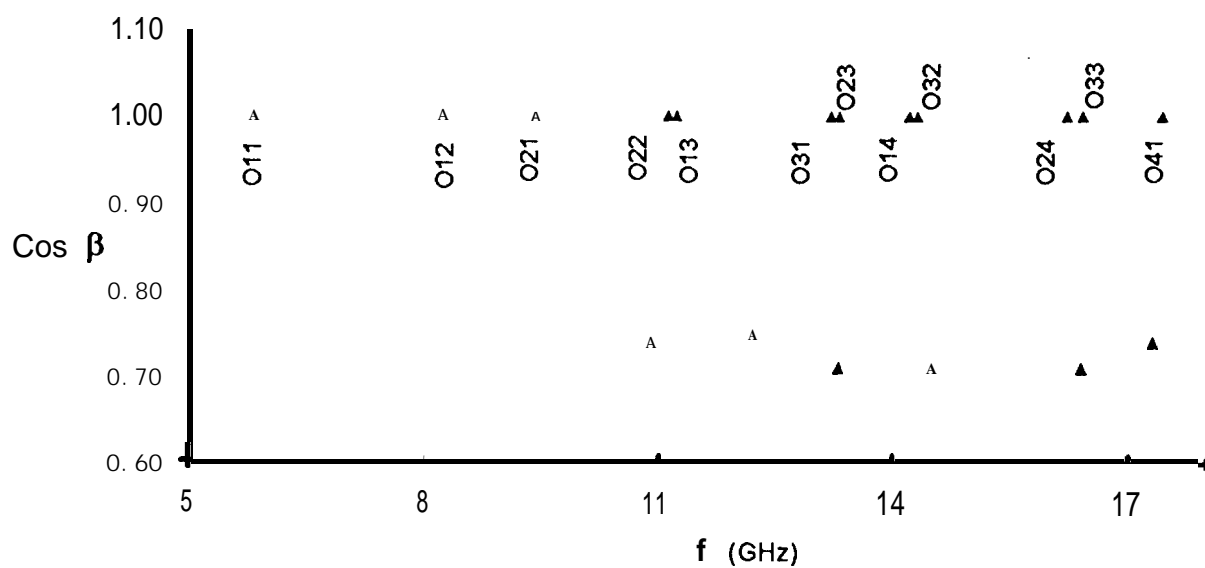


Figure 2. Finite element frequencies of modes obtained for the hollow cavity. The modes with cosines close to unity are physical, while those with smaller values are spurious.

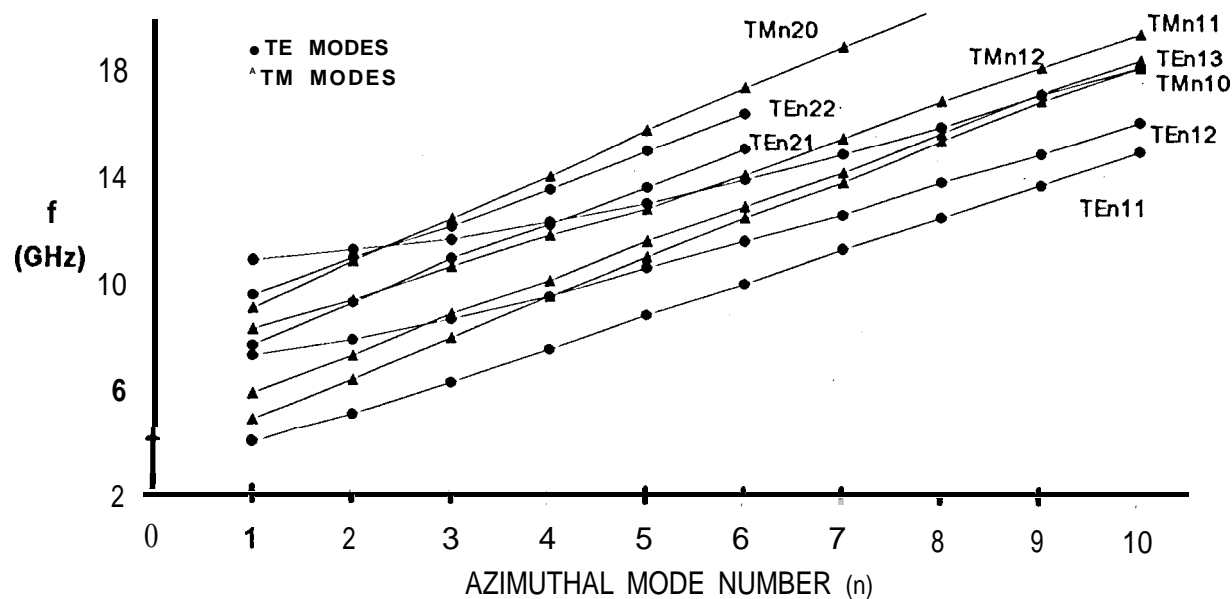


Figure 3. Sample families of modes obtained from the finite element analysis of the hollow Cavity with 100 quadrilateral elements.

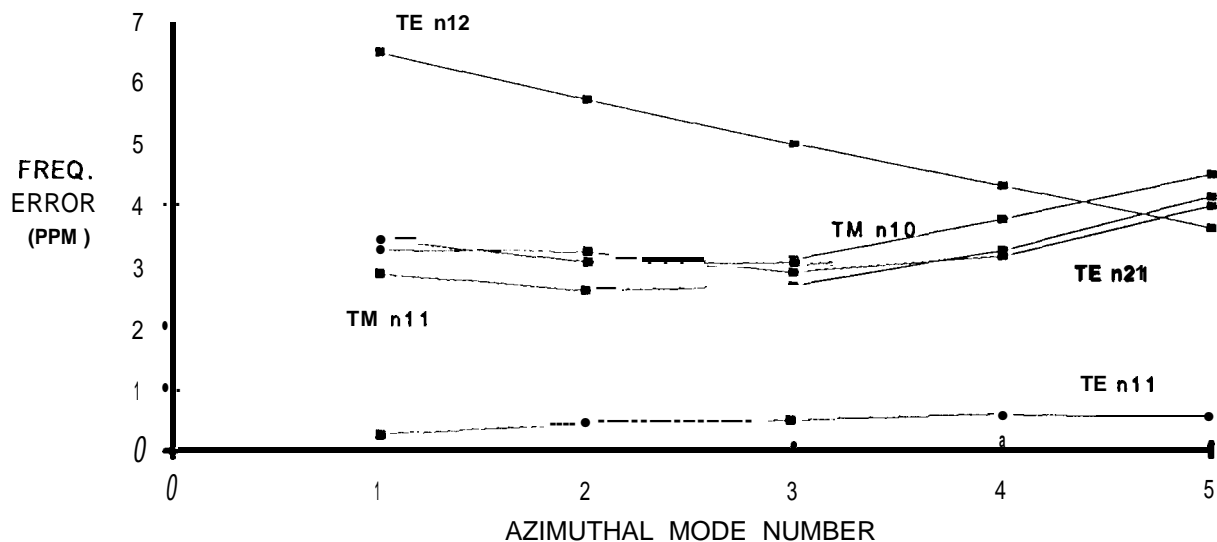


Figure 4. Frequency error for several mode families of coaxial resonator.

Somewhat higher accuracy was found when the method was applied to a coaxial cavity, where a more uniform geometry is obtained for elements near its geometrical center. The coaxial resonator had an outer radius of 5 cm, an inner radius of 2.5 cm, and a height of 5 cm. Figure 4 shows the difference in parts per million (PPM) between the finite element solution using 220 elements and the analytic solutions for various mode families. Frequency errors for the first five mode families are all less than 7 parts per million, with errors for the fundamental TE_{n11} mode family being less than 1 PPM.

V. Comparison to Measurements

The proposed finite element approach was also tested by solving for the resonant frequencies and modes of a cylindrical sapphire resonator experimentally studied by the Jet Propulsion Laboratory, Reference [5] includes details of the experimentation and of the measured frequencies for different families of modes.

Figure 5 illustrates the geometrical axisymmetric plane of the resonator tested. The sapphire material was held together by a copper core in the center and encapsulated inside a copper cylinder. The resonator was modeled using three finite element meshes comprising of eight-node elements of

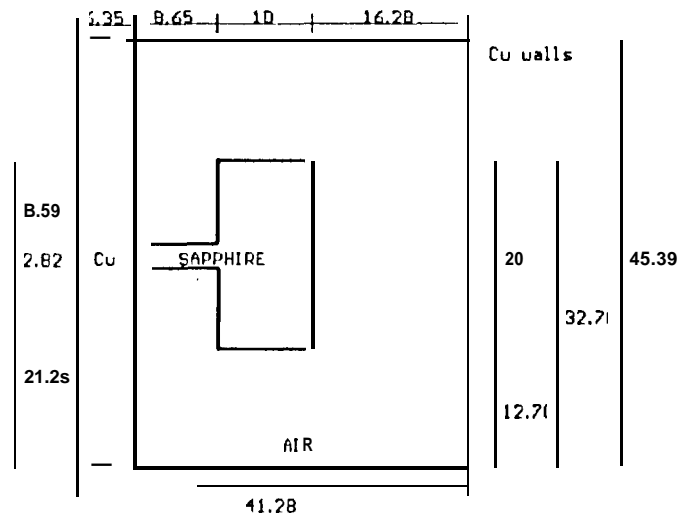


Figure 5. Dimensions (in mm) of sapphire resonator,

sapphire and air materials. The dielectric properties of the sapphire material were taken from Ref. [2] as $\epsilon_{rr} = \epsilon_{\phi\phi} = 9.407$ and $\epsilon_{zz} = 11.62$. The coarse mesh consisted of 62 nodes and 15 elements, the medium mesh of 193 nodes and 54 elements, and the finest mesh has 709 nodes and 216 elements. The perfect electric conductor boundary condition reflected in (4) was enforced at all metal boundaries of the finite element meshes. The **eigenvalue** solution of (18) was obtained for azimuthal order values ranging from 3 to 12. Each solution yielded a set of resonant frequencies with associated **eigenvectors**. The lowest frequency solution corresponded to the fundamental mode for that n^{th} azimuthal order.

Figure 6 shows the resonant frequencies of the fundamental family of modes WGH_{n11} for the three meshes with n values ranging from 3 to 12, illustrating convergence of the solutions as the finite element mesh was refined. The mode classification shown is based on the notation of Jiao, et al [6] for whispering-gallery 'modes. A finer mesh was not considered feasible due to computer memory limitations.

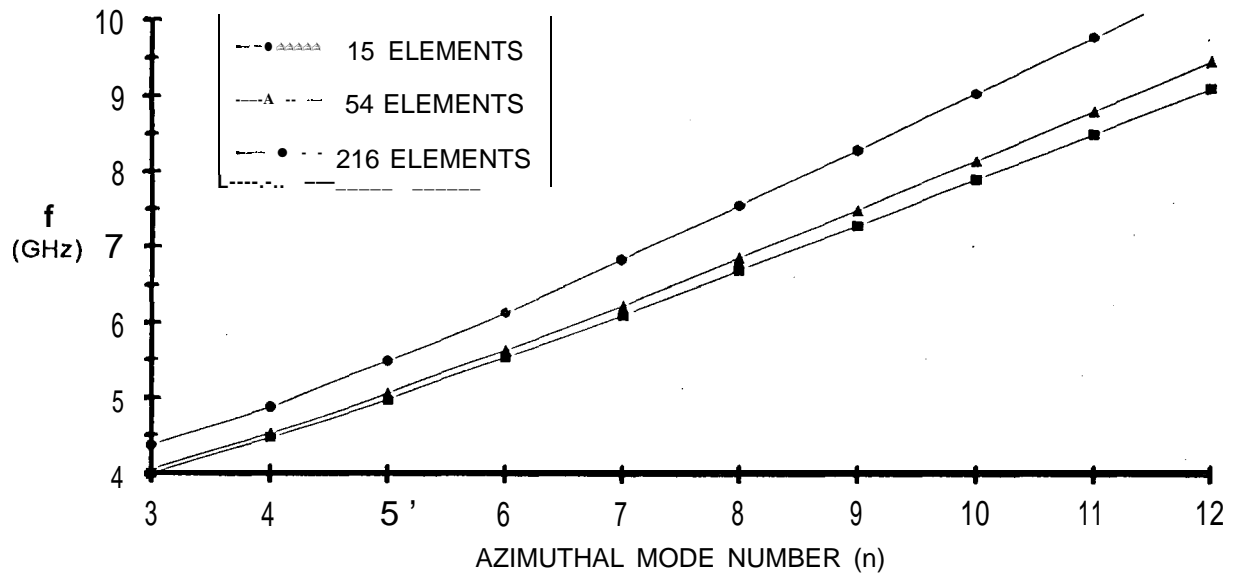


Figure 6. Convergence curves of the finite element frequency for the fundamental WGH_{n11} family in the sapphire resonator using different mesh sizes.

Figure 7 shows the frequencies of the families of modes that were identified and that matched with the frequency measurements made at the Jet Propulsion Laboratory [5]. The solid lines of the figure correspond to the finite element results and the dots are the measured values. From this figure it is observed, that the finite element results agree well with the measurements. The errors in the resonant frequencies of fundamental family WGH_{n11} modes, obtained from the three meshes, with respect to the measurements are listed in Table 1. Errors of the resonant frequencies of the rest of the families shown in Fig. 7, including uncertainties in ϵ , were all less than one percent.

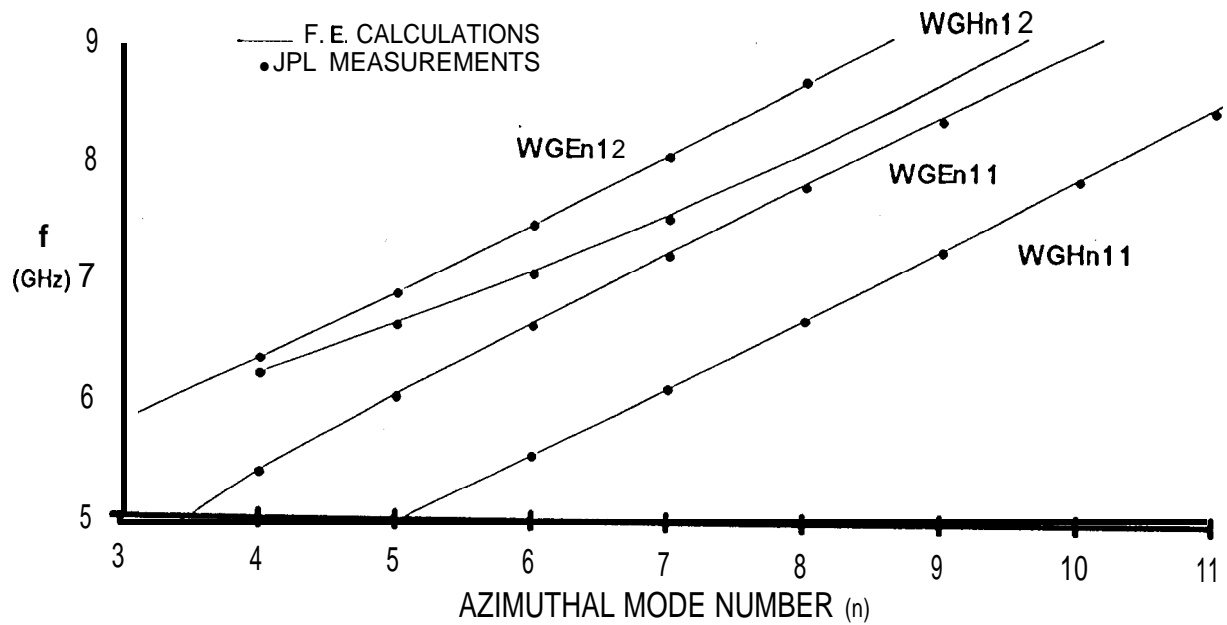


Figure 7. Comparison of resonant frequencies obtained from finite element analyses with measurements made on a cylindrical sapphire resonator,

Table 1. Error of Resonant Frequency of Fundamental Family WGH_{n11} with Respect to Experimental Measurements

Azimuthal Number n	Error (%)		
	Coarse Mesh	Medium Mesh	Fine Mesh
6	11.0	1.9	0.15
7	12.0	2.3	0.16
8	13.1	2.7	0.22
9	14.0	3.1	0.26
10	14.9	3.6	0.28
11	15.7	4.1	0.55

VI. Conclusions

A finite element method has been presented for treating a cylindrical resonator partially filled with an anisotropic dielectric as a two-dimensional finite element problem assuming harmonic oscillation for the field dependence in azimuth. This technique allows the first treatment of the technically interesting case of an anisotropic but axisymmetric dielectric mounted in a cylindrical conducting container. The method was first validated with a hollow, metallic, cylindrical resonator and with a coaxial cavity by comparing the numerically-obtained results with the exact analytical expressions. The method was then tested with a cylindrical sapphire resonator for which there are no exact solutions available. The numerical results obtained from the method were grouped by families of modes and the frequencies compared to experimental values obtained at the Jet Propulsion Laboratory. Excellent agreement was found for all the cases, thus indicating that the method is valid.

Acknowledgements

The authors wish to acknowledge the technical comments and discussions provided by Alfred R. Paiz and Lute Maleki from the Jet Propulsion Laboratory during the course of this research.

REFERENCES

- [1]. Kajfez, D. and P. Gillon, Eds., Dielectric Resonators, Artech House, Boston, 1986.
- [2]. Tobar, M.E. and A.G. Mann, Resonant Frequencies of Higher-Order Modes in Cylindrical Anisotropic Dielectric Resonators, IEEE MTT-S International Microwave Symposium Digest, pp. 495-498, 1991.
- [3]. Konrad, A., Vector Variational Formulation of Electromagnetic Fields in Anisotropic Media, IEEE Trans. Microwave Theory and Techniques, Vol. MTT-24, No. 9, pp. 553-559, 1976.
- [4]. Wang, J.S. and N. Ida, Eigenvalue Analysis in Anisotropically Loaded Electromagnetic Cavities Using "Edge" Finite Elements, IEEE Trans. on Magnetics, Vol. 28, No. 2, pp. 1438-1441, 1992.
- [5]. Dick, G.J. and J. Saunders, Measurements and Analysis of a Microwave Oscillator Stabilized by a Sapphire Dielectric Resonator for Ultra-Low Noise, IEEE Trans. on Ultrasonics, Ferroelectrics, and Frequency Control, Vol. 37, No. 5, pp. 339-346, 1990.
- [6]. Jiao, X., P. Guillon, and L.S. Bermudez, Resonant Frequencies of Whispering-Gallery Dielectric Resonator Modes, IEEE Proceedings, Vol. 134, Pt. H, No. 6, pp 497-501, 1987.
- [7]. Davies, J. B., F.A. Fernandez, and G.Y. Phileppou, Finite Element Analysis of All Modes

in Cavities with Circular Symmetry, IEEE Trans. Microwave Theory & Techniques, Vol. MTT-30, No. 11, pp. 1975-1980, 1982.

- [8]. Koshiba, M., K. Hayata, and M. Suzuki, Improved Finite Element Formulation in Terms of the Magnetic Field Vector for Dielectric Waveguides, IEEE Trans. on Microwave Theory and Techniques, Vol. MTT-33, No. 3, pp. 227-233, 1985.
- [9]. Zienkiewicz, O.C. and Taylor, R. L., The Finite Element Method, 4th Ed., Vol. 1 Basic Formulation and Linear Problems, McGraw-Hill, London, 1989.
- [10]. Conte, S.D. and C. De Boor, Elementary Numerical Analysis: an Algorithm Approach, 3rd. Ed., McGraw-Hill, NY, 1980.